Neuron, Vol. 47, 607–620, August 18, 2005, Copyright ©2005 by Elsevier Inc. DOI 10.1016/j.neuron.2005.07.016

Contrast Adaptation and Representation in Human Early Visual Cortex

Justin L. Gardner,[1,2,*] Pei Sun,[1] R. Allen Waggoner,[1] Kenichi Ueno,[1] Keiji Tanaka,[1] and Kang Cheng[1]
[1]Laboratory for Cognitive Brain Mapping
RIKEN Brain Science Institute
2-1 Hirosawa, Wako
Saitama 351-0198
Japan
[2]Center for Neural Science
and Department of Psychology
New York University
New York, New York 10003

Summary

The human visual system can distinguish variations in image contrast over a much larger range than measurements of the static relationship between contrast and response in visual cortex would suggest. This discrepancy may be explained if adaptation serves to recenter contrast response functions around the ambient contrast, yet experiments on humans have yet to report such an effect. By using event-related fMRI and a data-driven analysis approach, we found that contrast response functions in V1, V2, and V3 shift to approximately center on the adapting contrast. Furthermore, we discovered that, unlike earlier areas, human V4 (hV4) responds positively to contrast changes, whether increments or decrements, suggesting that hV4 does not faithfully represent contrast, but instead responds to salient changes. These findings suggest that the visual system discounts slow uninformative changes in contrast with adaptation, yet remains exquisitely sensitive to changes that may signal important events in the environment.

Introduction

Our visual system is sensitive to many orders of stimulus strength, seemingly capable of distinguishing mountains in the mist as effortlessly as the stripes on a zebra. This ability is all the more amazing given that neurons in the visual pathways are only sensitive to a small range of stimulus strengths. In the cortical visual system, image contrast is the visual property most associated with stimulus strength. Indeed, increasing stimulus contrast makes things more visible, and both single-unit recordings (Albrecht and Hamilton, 1982; Anzai et al., 1995; Dean, 1981; Tolhurst et al., 1981) and human imaging (Avidan et al., 2002; Boynton et al., 1999, 1996; Heeger et al., 2000; Kastner et al., 2004; Logothetis et al., 2001; Tootell et al., 1995) find monotonically increasing activity in the primary visual cortex (V1) with increases in stimulus contrast. However, neurons in V1 do not respond proportionally to all ranges of contrast; they display a sigmoidally shaped contrast response curve (Albrecht and Hamilton, 1982), which is most sensitive to contrast differences in the midrange of the curve and much less sensitive to contrasts above or below this range.

Adaptation mechanisms have been proposed as a possible explanation of how the visual system overall can be sensitive to such a wide range of image contrasts while the individual neurons have only a limited dynamic range. Prolonged exposure to a stimulus results in a wide range of visual adaptation effects (e.g., Blakemore and Campbell, 1969). These types of perceptual adaptations are paralleled by decreases in firing rates of neurons in V1 (Dean, 1983; Hammond et al., 1985; Movshon and Lennie, 1979; Vautin and Berkley, 1977). If these decreases in neuronal response were generalized to all contrast levels, a response gain decrease, they would be expected to have a detrimental effect on vision, simply reducing sensitivity to all contrasts. However, single-unit experiments in striate cortex of anesthetized cats (Bonds, 1991; Ohzawa et al., 1982, 1985; Sclar et al., 1985), monkey and prosimian V1 (Allison et al., 1993; Carandini et al., 1997; Sclar et al., 1989), and monkey middle temporal area (MT; Kohn and Movshon, 2003) have revealed that adaptation to contrast results in mostly horizontal shifts of contrast response functions. This finding, a contrast gain change, reflects a more beneficial process for vision in that it serves to recenter contrast response curves around the time-averaged contrast level, allowing these neurons to encode contrasts that are relevant to the scene being viewed.

Despite these provocative findings in anesthetized animals, it is not known if these changes occur in the human visual system, let alone whether they represent a general mechanism across visual areas. Imaging studies provide conflicting reports on whether contrast adaptation can be detected in human visual cortex (Engel and Furmanski, 2001) or not (Kastner et al., 2004); also, how contrast response functions change with adaptation has not yet been investigated. Beyond V1, only one study (Kohn and Movshon, 2003) has examined how contrast response functions change with adaptation in monkey MT. Despite this lack of physiological evidence in humans, psychophysical measurements of contrast discrimination thresholds have been found to change with adaptation in a way that is consistent with contrast gain and not response gain changes (Greenlee and Heitger, 1988). By imaging early visual cortex in awake humans, using an event-related functional magnetic resonance imaging (fMRI) technique, we have established that in V1, V2, and V3, there are profound contrast gain changes that are consistent with psychophysics and confer a beneficial effect on human vision.

We also found a basic difference between the response to contrast changes of human V4 (hV4) and earlier visual cortex, which has not been reported in either monkey electrophysiology or fMRI experiments; hV4 responded positively to contrast changes regardless of the sign of the change. This result signals a fundamental shift in visual processing between hV4 and earlier visual cortical areas. While slowly changing or

*Correspondence: justin@cns.nyu.edu

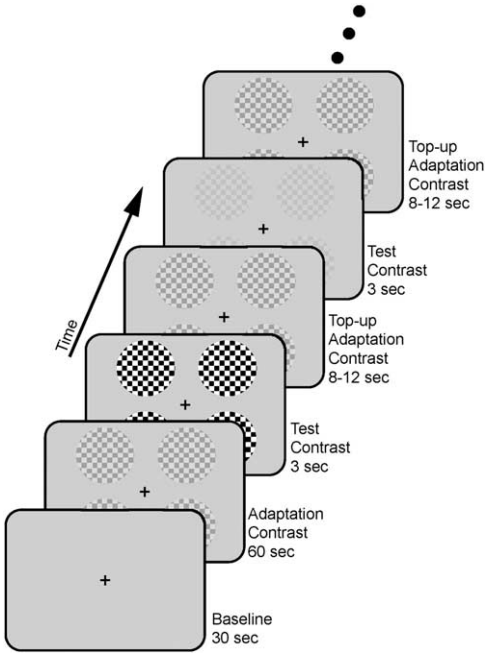

Figure 1. Visual Stimulation Paradigm for Event-Related Contrast Adaptation Experiment

static contrast levels are unlikely to signal biologically relevant events, changes in contrast, regardless of whether they are increases or decreases, may signal important events to which our visual system should be sensitive. Contrast adaptation is a process by which neurons adjust to slowly changing or static contrast levels, thus reducing our sensitivity to these uninformative features of the visual world. The response property of hV4 that we found is the expected signature of a process that counterbalances slow adaptation to static contrast by being sensitive to the salience of dynamic changes.

Results

Measurements of Contrast Response Functions with an Event-Related fMRI Paradigm

We measured blood oxygen level-dependent (BOLD) contrast response functions for three different levels of adaptation contrast (6.25%, 12.5%, and 25%), using an event-related stimulus paradigm (Figure 1). After an initial 30 s baseline phase, we presented the adaptation stimulus to the subject for 60 s. During the whole experiment, we instructed the subject to perform a detection task on the fixation cross, to keep fixation centered and to provide a control for attentional state. We tested contrast response by incrementing or decrementing the contrast by 1 or 2 octaves (an octave being a doubling) for 3 s. Contrast was the only aspect of the stimulus that we changed during these periods. After each test contrast, we readapted the subject with the adaptation contrast for 8–12s. This stimulus paradigm, adapted from electrophysiological experiments (Ohzawa et al., 1982), was used because both the readaptation (or top-up) contrasts and the balancing of contrast increments and decrements serve to keep the time-averaged contrast during the experiment at the adaptation level.

Examination of the time course from a representative voxel taken from one subject's retinotopically mapped V1 shows the BOLD response to the various events in our experiment (Figure 2A). During the baseline phase, the time course is flat, with some fluctuations. Soon after we turn on the adaptation stimulus (yellow arrow), the time course displays a rapid rise followed by a slower decay. We interpret this decay as a signature of neural adaptation and analyze it in detail in Figure 6. Following this initial adaptation period, the time course exhibits transient peaks following the times that we increased the contrast by 1 or 2 octaves (green and magenta arrows, respectively). Following the times when we decrease the stimulus contrast by 1 or 2 octaves (purple and cyan arrows, respectively), there are transient dips.

To use these transient peaks and dips following contrast increments and decrements as a measure of the contrast response, we first estimated the average response to each contrast, using a deconvolution procedure (Figure 2B). This procedure, without assuming a shape for the hemodynamic response, takes a stimulus-triggered average and assumes that any overlap in responses results in linear combination (Boynton et al., 1996; Dale and Buckner, 1997). After an ~3 s delay following increments in stimulus contrast, these hemodynamic responses exhibited a large positive peak followed by a longer lasting negative undershoot, classic features of the hemodynamic response (Kruger et al., 1996). These hemodynamic responses were scaled by the test contrast, displaying a larger response for 2 octaves than for 1 octave (magenta and green curves, respectively). Conversely, hemodynamic responses to transient decrements in contrast displayed a transient decrease in the BOLD response that also scaled with the magnitude of contrast change (purple and cyan curves).

We developed a procedure to determine the significance of event-related activations on a voxel-by-voxel basis without recourse to the more usual practice of averaging together the response of voxels in a region of interest (ROI) defined by activations from another experiment. We first calculated the amount of variance in the raw time course that was accounted for by the hemodynamic responses such as the ones shown in Figure 2B. This value, r^2, is equal to 0 if stimulus-locked events in the time course do not account for any of the variance, and $r^2 = 1$ if these events account for all of the variance. The distribution of r^2 for all voxels in a volume for one experiment (Figure 3A inset, green bars, mostly obscured by blue bars), shows a broad distribution of values with a mean of 0.09, reflecting the fact that the majority of voxels in the volume are not being activated by our stimulus and therefore have low r^2 values. To determine which of these r^2 values were higher than can be expected by chance, and were therefore significantly activated by our stimulus, we randomly shuffled stimulus times and recomputed a distribution of r^2 values (blue bars). An expansion of the tail of the real and randomized distributions (Figure 3A) reveals that the distribution of real r^2 values contains values

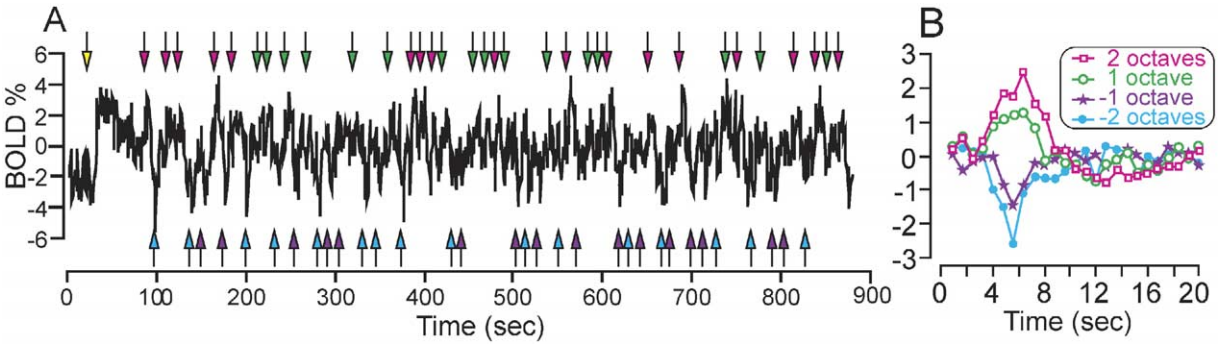

Figure 2. Example Time Course from a Single Voxel in Retinotopically Defined V1

(A) BOLD response as a function of time. Yellow arrow marks the time when the adaptation stimulus was first presented. Green and magenta arrows indicate when test contrasts 1 or 2 octaves above the adaptation contrast were presented. Purple and blue arrows mark test contrast presentations 1 or 2 octaves below the adaptation contrast. 0% BOLD is set to the mean level after the 60 s adaptation period.

(B) Deconvolved responses to each stimulus contrast as a function of time from the beginning of the presentation of each stimulus contrast.

much higher than those predicted by chance in the randomized distribution.

Maps of r^2 values (Figure 3, bottom right) with a cutoff chosen on the basis of the randomized distribution (red arrowhead, Figure 3A) to produce a false alarm probability of $p = 0.001$ validate this measure of activation in two ways: (1) Voxels that have r^2 values higher than those expected by chance were clustered in parts of the early visual cortex where they were expected to be based on retinotopy; and (2) the hemodynamic response functions of these voxels were all of the classic form (Figures 3B–3D). At a cutoff of $p = 0.001$, the image in Figure 3 (cropped to 48 × 48 voxels) is expected to have 2.3 voxels falsely classified as activated and has two obvious false positives located outside the brain; (the full image [64 × 64 voxels] is expected to have 4.1 false positives and has six).

Using this voxel-by-voxel measure of significance, we constructed contrast response functions from the hemodynamic responses of significantly activated voxels ($p < 0.001$). We first calculated the response to the adaptation contrast as the difference between the mean level during the experiment after the adaptation period and the mean level during the baseline period. The rationale for this measure was that for the majority of time during the experiment, the adaptation contrast was presented, and the test stimuli were balanced for contrast increments and decrements, thus making the time-average contrast the same as the adaptation contrast (see below for discussion on possible sources of

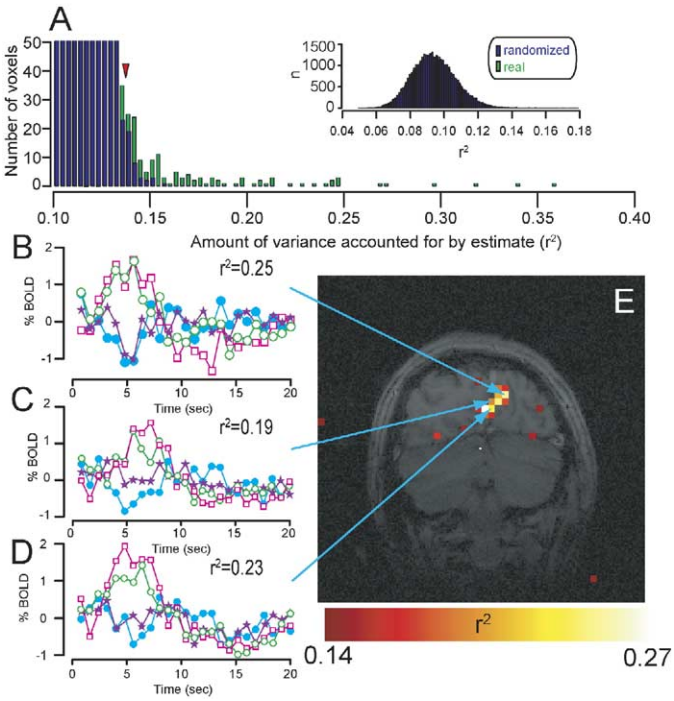

Figure 3. The Amount of Variance Accounted for by Stimulus Time-Locked Events (r^2) Is a Reliable Indicator of Activated Voxels

(A) Distribution of r^2 values obtained for the real data (green) and when the stimulus times were randomly shuffled (blue). Inset shows the distribution for all voxels in the volume, and the main graph shows only the tail. Red arrowhead marks the r^2 cutoff value chosen on the basis of the randomized distribution for this experiment.

(B–D) Examples of hemodynamic responses from voxels with r^2 values higher than the cutoff value, which are in retinotopically expected areas and show classic hemodynamic responses (same conventions as described for Figure 2B).

(E) Coronal image with color overlay indicating r^2 values.

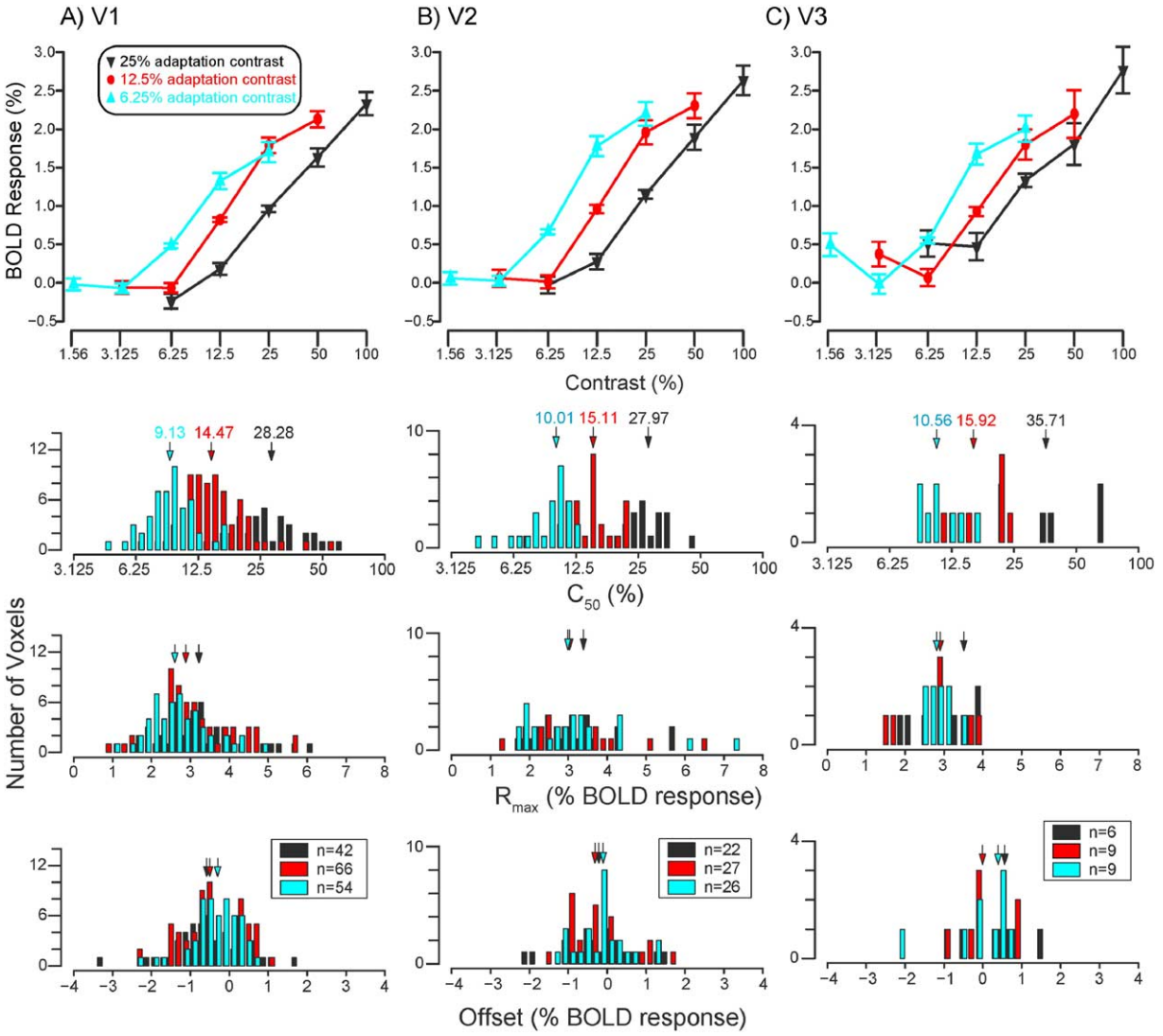

Figure 4. Contrast Response Functions for Different Adaptation Levels and in Different Visual Areas

The top row of (A–C) shows contrast response functions (mean ± SEM) constructed for voxels in V1, V2, and V3, averaged over all subjects. 0% BOLD is the mean response during the baseline period of the experiment. The bottom three rows show distributions of c_{50}, R_{max}, and offset parameters of fits of contrast response functions performed on a voxel-by-voxel basis. Arrows indicate the mean values of distributions.

error). We then fit gamma functions to each of the hemodynamic responses (Figure 2B) and used the peak of this function as the response to each of the test contrasts. These points were then plotted above and below the response to the adaptation contrast. We discarded voxels with a response amplitude higher than 5%, as these were likely due to signals from large draining veins, and voxels in which the amplitude of the gamma fit was not adequately constrained by the data (variance of the amplitude parameter estimate >50%).

Horizontal Shifts of Contrast Response Functions

We plotted contrast response functions in this way for each of the three adaptation contrasts (6.25%, 12.5%, and 25% contrast; cyan, red, and black curves, respectively; Figures 4A–4C, top row). Each function shows the mean and SEM of the contrast response function constructed from all significantly activated voxels ($p < 0.001$) taken from eight experiments conducted in five different subjects (two subjects were tested multiple times). The number of voxels used to construct the curves for 6.25%, 12.5%, and 25% adaptation for V1 was 51, 74, and 77, respectively. For V2 there were 34, 46, and 39 voxels, and for V3 there were 11, 15, and 22. Examination of these curves reveals that the primary effect of adaptation is to shift the contrast response curves horizontally to the right with higher adaptation contrasts. This trend can be seen for curves generated for V1 (Figure 4A), as well as for V2 and V3 (Figures 4B and 4C).

We next used a voxel-by-voxel analysis to quantitatively examine the shifts in contrast response functions. For this analysis, we fit a sigmoidal function (Albrecht

and Hamilton, 1982; Naka and Rushton, 1966) to contrast response functions constructed separately for each activated voxel at each adaptation level. In this analysis, we required that a voxel be activated at $p < 0.001$ for all adaptation contrasts tested (which were three contrasts, except for two of the eight experiments, in which we collected only the data for 6.25% and 12.5% adaptation contrasts for one and only the 12.5% adaptation contrast for the other). We adjusted three parameters in the fit; the center (c_{50}), the amplitude (R_{max}), and the offset. These curves fit our data satisfactorily, accounting for 93% of the variance, on average. The distributions of the c_{50} parameter for different adaptation levels in V1 (Figure 4A, second row,) show a systematic shift toward higher values with higher adaptation contrasts. In fact, the means of the distributions closely track the adaptation contrasts for which they were obtained, indicating that the center of the contrast response curves shifts near the adaptation contrast. The distribution of R_{max} (Figure 4A, third row) shows a trend for larger amplitude contrast response functions with higher adaptation levels, but this effect did not generally reach statistical significance (see below). There were no systematic differences in the distribution of offsets (bottom row) for different adaptation levels. The effects of adaptation on these three parameters of the sigmoidal fits to the contrast response functions were qualitatively similar for all three visual areas.

To test the statistical significance of the qualitative results reported above, we used a nested ANOVA in which we tested the difference across adaptation conditions among the data for each voxel nested inside groups collected on different days from different subjects. This analysis confirmed the difference across adaptation conditions of the c_{50} parameter for V1–V3 ($p < 0.001$) and found no significant difference in means for the offset and R_{max} parameters (all $p > 0.7$), except for a difference in R_{max} for V2 ($p = 0.034$). Intersubject variations were not significant except for the offset parameter for some areas ($p = 0.0034$, $p = 0.022$, $p = 0.1$, V1, V2, and V3 respectively) and for the c_{50} parameter only in V3 ($p < 0.001$, all other $p > 0.3$). These results confirm that the main difference in contrast response functions across adaptation conditions is a shift in the horizontal location (c_{50}) with differences in the amplitude (R_{max}) reaching borderline significance in one case. Furthermore, there was only a modest amount of intersubject variation, primarily for the offset parameter.

Horizontal Shifts of Contrast Response Functions Regardless of Voxel Selection

We next explored the consequences of changing the voxel selection criteria from the fairly restrictive cutoff used in Figure 4 to one that includes all voxels in the ROI defined from retinotopic mapping. We did this by systematically changing the r^2 cutoff value for including voxels in the construction of the contrast response functions in V1–V3, using cutoff values of 0.11, 0.10, 0.09, 0.08, 0.05, and 0.0 (Figure 5, in descending order of color saturation). The final cutoff value corresponds to inclusion of all of the voxels defined from the retinotopic ROI—942, 715, and 633 voxels, respectively, for V1, V2, and V3. Contrast response functions in V1 and V2 still maintained horizontal shifts with adaptation even when all voxels in the retinotopic ROI were included. However, as more voxels that were not activated by the stimulus were included in the analysis, the contrast response functions become correspondingly more flat. This effect is most pronounced for area V3, which had the least number of activated voxels, flattening the curves to such an extent that the consequences of adaptation on contrast response were obscured.

To quantitatively assess whether the method of selecting voxels for analysis affects our results, we performed a nested ANOVA analysis (similar to that above) on all voxels from V1–V3 defined using the ROI method. The difference in c_{50} was significant for V1–V3 ($p < 0.001$), and no other parameters showed significant differences ($p = 0.094$ for R_{max} in V1; all other $p \geq 0.4$). Intersubject variations were only significant for the offset parameter for some areas ($p < 0.001$, $p = 0.23$, and $p = 0.050$, V1, V2, and V3, respectively), the c_{50} parameter, for V3 ($p < 0.001$), and the R_{max} parameter, for V2 ($p = 0.017$; all other $p > 0.5$). These results indicate that our primary observation of horizontal shifts of c_{50} as a consequence of contrast adaptation is largely independent of the voxel selection.

Possible Sources of Error in the Construction of Contrast Response Functions

In estimating the response to the adaptation contrast, we used the mean during the experiment, which may be subject to two sources of error. First, though the contrast increments and decrements were balanced on a log scale, the neural responses may not be completely balanced, thus contaminating the estimate of the response. Second, our high-pass filter, though set to be quite conservative, could have filtered out differences in adaptation levels. To test whether these factors might substantially change our results, we recalculated the response to the adaptation contrast as the average of the last 15 time points acquired in the last 12 s of the adaptation period from the data before temporal filtering. We expected the response in this epoch to be near the steady-state level, but not to be contaminated by responses to test stimuli. Using the same nested ANOVA approach as above, we confirmed that this analysis produced equivalent results. Differences in the c_{50} parameter across adaptation conditions were significant ($p \leq 0.015$, V1–V3), with the slightly larger p values presumably reflecting the noisier response estimation without filtering. The offsets and R_{max} parameters were all nonsignificant across adaptation conditions ($p > 0.7$) except for the R_{max} parameter for V2 ($p = 0.033$). Employing the full ROI-based method and including all voxels regardless of their r^2 value again resulted in significant differences for the c_{50} parameter for all areas ($p \leq 0.011$) and nonsignificance for differences of the offsets and R_{max} parameters ($p > 0.3$) except for the R_{max} parameter for V3 ($p = 0.024$).

Time Course of Adaptation

We next examined the time course over which the BOLD measurements adapted by examining the initial 60 s response when the adaptation stimulus was first

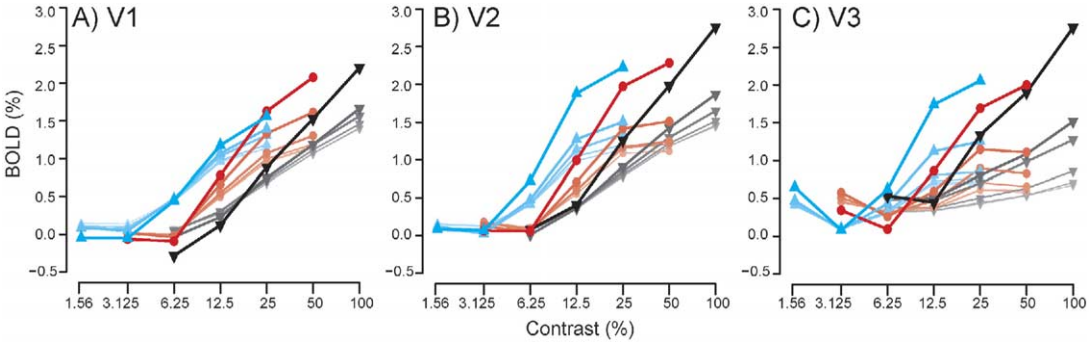

Figure 5. Change in Contrast Response Functions with Different r^2 Cutoffs

Contrast response functions for V1, V2, and V3 are shown in (A), (B), and (C), respectively. Curves are constructed with voxels exceeding a cutoff r^2 value, as in Figure 4 (most saturated colors and thickest lines) and with cutoff values 0.11, 0.1, 0.09, 0.08, 0.05, and 0 (in descending order of color saturation and line thickness). The curve with cutoff value 0 is equivalent to an ROI-based approach since it includes all voxels in the ROI.

turned on (indicated by the yellow arrow, Figure 2A). The average response for voxels in each visual area shows an initial rise as the adaptation stimulus is turned on, followed by a slower decay as the signal adapts. We fit these responses from the time of peak to the end of the adaptation period with a decaying exponential function (solid curves, Figures 6A–6C). These functions made reasonable fits to the data accounting for 57%–84% of the variance in V1; 50%–70%, in V2; and 24%–63% of the variance in V3. The time constants for the adaptation effect show that this effect has a timescale on the order of tens of seconds, with the median time constants from V1–V3 being 14.42 s (18.03 ± 3.19 s, mean ± SEM).

Previous fMRI experiments have used block design experiments to test contrast sensitivity (Avidan et al., 2002; Kastner et al., 2004; Tootell et al., 1995), in which the response to each contrast is typically measured over many seconds. Block design experiments may therefore be more sensitive to the adapted response near the end of adaptation (red arrow, Figure 6A), rather than the initial response to the contrast before adaptation (black arrow, Figure 6A). We examined the difference in contrast sensitivity that these two measures showed, by plotting the initial peak (Figure 6, right column, black squares) and the adapted response taken as the mean during the experiment (red circles). The range of response was much greater for the preadaptation data than for the postadaptation data. For example, when the stimulus was 6.25% contrast versus 25% contrast, the difference in response for V1 was 1.09% of BOLD response. After adaptation, this difference was only 0.28%. Taking the ratio of these values reveals that the contrast sensitivity was 3.88 times greater before adaptation. Contrast sensitivity measured in this way was 3.10 and 3.37 times greater for V2 and V3, respectively.

Positive Responses to Contrast Decrements in hV4

We found that the responses to contrast decrements in hV4 were fundamentally different from the responses in earlier visual cortex. While earlier visual areas all showed decreases in response when contrast was decremented, voxels in hV4 responded to both contrast decrements and contrast increments with positive responses, a single-voxel example of which is shown in Figure 7A. These responses, averaged over voxels, led to flatter contrast response functions than did those in earlier visual areas (Figure 7B), though too few voxels survived the criteria ($p < 0.001$; an average of four voxels in each experiment) to make the curves interpretable. When we opened up the criteria to accept false positive probabilities of 0.005, 0.01, 0.02, 0.05, and 0.1 (r^2 from 0.14 to 0.11, in descending order of color saturation; Figure 7C), as well as the full hV4 ROI which had an average of 106 voxels, we found that the contrast response functions began to look more U-shaped, rather than S-shaped, due to the positive responses to contrast decrements (Figure 7C). To further examine these positive responses, we conducted another set of experiments that had two purposes. The first purpose was to increase the yield of voxels in hV4 to confirm that positive responses to contrast decrements indeed constituted a property of hV4. Higher visual areas successively take up less cortical surface (Dougherty et al., 2003) and are farther away from the surface coil, thus yielding fewer voxels for our analysis and, consequently, the larger error bars in Figures 4 and 7. We therefore reduced our field of view from 24 × 24 cm^2 to 20 × 20 cm^2 to obtain voxels with smaller in-plane resolution (3.125 × 3.125 mm^2). We also tested only two relatively large test contrasts, 87.5% and 12.5%, from an adaptation contrast of 50%, in an effort to elicit large responses. The second, and more fundamental, purpose of this experiment was to test how rapidly contrast decrements had to occur to evoke positive responses from hV4. We therefore slowly changed the stimulus contrast (half a period of a sinusoid modulation), rather than presenting it as an abrupt change (Figure 8A, insets). These sinusoidal modulations were presented for 12.5, 8.3, 6.25, 4.167, or 3.125 s. Each block contained a contrast increment and decrement of one length presented at least 12 times each. The stimulus sequence was analogous to that in the first experiment (Figure 1), except that the initial adaptation period was 40 s.

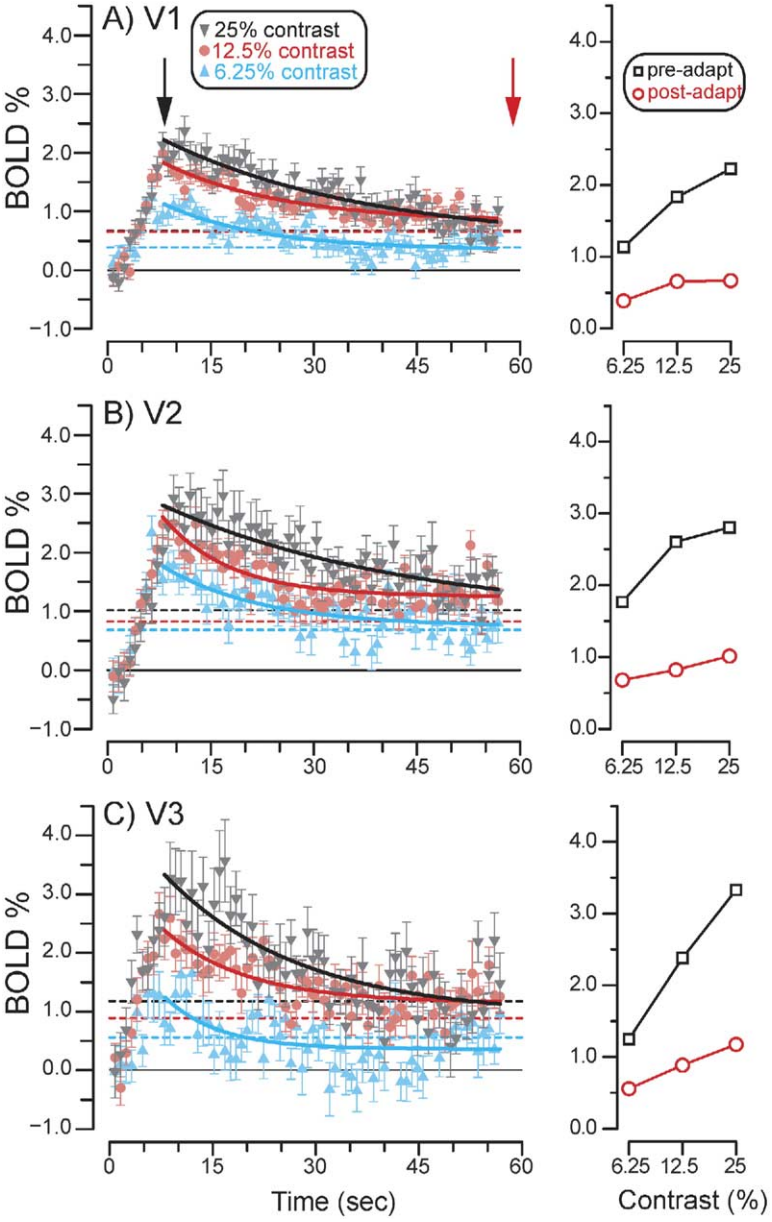

Figure 6. Analysis of the Rate at which Adaptation Affects BOLD Responses

The left panels in (A), (B), and (C) show the responses averaged over subjects for the first 60 s of BOLD response after the adaptation stimulus is first shown, for V1, V2 and V3, respectively. The black arrow indicates the time of the initial response that is used to calculate contrast sensitivity shown in the right column (open black squares). The red arrow marks the end of the adaptation period. The open red circles in the right column plot the contrast sensitivity as the average response during the experiment. Error bars indicate the mean ± SEM.

As expected, we found that V1–V3 responded with positive responses to contrast increments (top row, Figures 8A–8C) and negative responses to contrast decrements (middle row). These positive and negative responses scaled appropriately with the stimulus lengths (magenta, cyan, blue, red, and black traces, in ascending order of durations). In contradistinction, hV4 exhibited positive responses regardless of whether the contrast was incremented (Figure 8D, top row) or decremented (middle row). We note that one response (to the shortest length) in V3 (magenta curve, middle row, Figure 8C) showed an early positive response to a contrast decrement. However, the error bars on the positive portion of this response suggest caution in the interpretation of these data without further replication.

One puzzling aspect of these responses in hV4 is that as contrast is decremented, the visual input to hV4 from V1–V3 is decreased and would be expected to result in a lower response in hV4. By closely examining the response in hV4, we found evidence that the initial positive hV4 response to contrast decrements is followed by a slower negative response. This can be appreciated by directly comparing the positive and negative responses (bottom row, Figure 8D) for the longest duration (12.5 s) of contrast change (solid line indicates a difference-of-gammas fit). The response to contrast decrements (red trace) is initially positive, but then ends with a large negative component. In principle, this negative response could be a poststimulus undershoot (Kruger et al., 1996), attributable to a lagged blood volume effect (Buxton et al., 2004; Mandeville et al., 1998), and not a decrease in neural firing. If this were the case, we would expect this negative portion of the response to scale with the initial positive response. In particular,

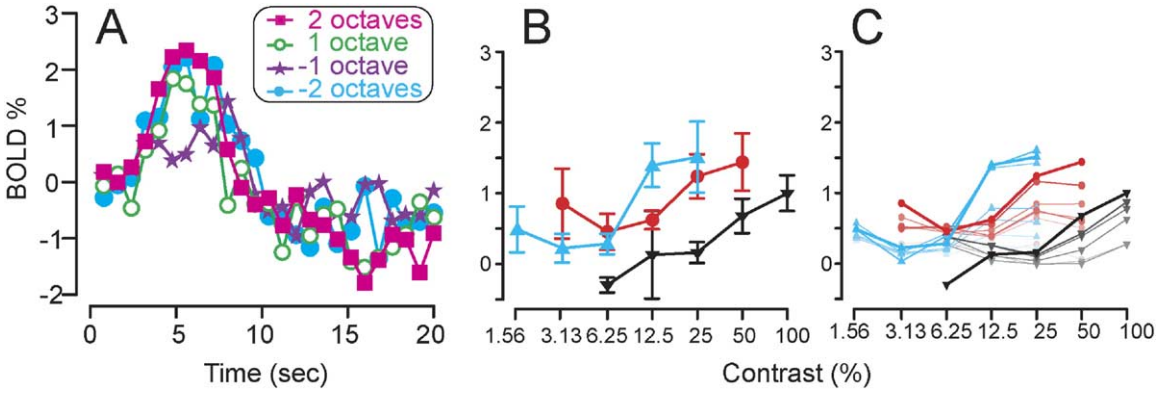

Figure 7. Responses to Contrast Decrements in hV4 Were Positive rather than Negative

(A) Hemodynamic responses to test contrasts for a representative voxel in hV4 (same conventions as those in Figure 2B).

(B) The average contrast response function with standard errors constructed for voxels in hV4 with the same criteria as those in Figure 4 ($p < 0.001$).

(C) Curves constructed from voxels with $p < 0.001$, $p < 0.005$, $p < 0.01$, $p < 0.02$, $p < 0.05$, and $p < 0.10$ and for the full ROI ($r^2 \geq 0.136$, $r^2 \geq 0.128$, $r^2 \geq 0.124$, $r^2 \geq 0.120$, $r^2 \geq 0.114$, and $r^2 \geq 0.109$, and 0, respectively) in descending order of color saturation and line thickness.

the negative component should be the same magnitude or smaller than the negative component of the response to the contrast increment (black trace), which has a larger initial positive response. That it is not suggests that the negative component is not simply a poststimulus undershoot, but may be due, in part, to a decrease in neural response after the initial increase to the contrast decrement. For all five stimulus durations, the negative component of the response was more negative than that in the positive response; on average, the difference in the minimum of the fits was 0.28% of BOLD response ($p < 0.01$, different from 0; Student's t test).

Discussion

We measured contrast response functions in human early visual cortex after contrast adaptation and found primarily horizontal shifts that nearly recenter these curves on the adapting contrast. While these horizontal shifts of contrast response functions were evident for V1–V3, hV4 showed a qualitatively different response to contrast decrements. Earlier cortex showed positive responses to contrast increments and negative responses to contrast decrements, but hV4 showed positive responses regardless of whether contrast was incremented or decremented.

Methodology

To test contrast response without significantly altering the adaptation state itself, it was imperative to use brief test stimuli in an event-related design. We implemented an analytical technique that did not make assumptions about the shape of the hemodynamic response and used the event-related responses themselves to determine activations. We believe that this technique was critical for our measurements, not simply because it allowed us to test contrast sensitivity without inducing significant adaptation, but because it allowed us to make measurements on a voxel-by-voxel basis. Event-related experiments often average together the responses of all voxels identified from a separate localizer. This tends to include noisy voxels not activated in the event-related experiment, thus reducing the signal. Our technique allows us to analyze only voxels that are significantly activated in the event-related paradigm, thus improving the quality of the signal that we measure.

Possible Mechanisms of Adaptation

Adaptation is unlikely to be simply a passive consequence of an inability to maintain high firing rates due to a lack of metabolic capacity, i.e., neural fatigue, as it confers beneficial properties on visual processing. Moreover, adaptation is associated with a tonic hyperpolarization in V1 neurons (Carandini and Ferster, 1997; Sanchez-Vives et al., 2000b) that may be attributable to synaptic depression (Adorjan et al., 1999; Chance et al., 1998; Finlayson and Cynader, 1995) or Ca^{2+}- and Na^{+}-activated K^{+} currents (Sanchez-Vives et al., 2000a), suggesting that it is an active process regulated by the cortex. Our data suggest that this active process of adaptation also serves to reset the metabolic baseline, producing less demand for static stimuli and thus reserving resources to sustain higher levels of activity necessary to encode changes in contrast. This suggestion is based on the indirect relationship between the BOLD signal and changes in metabolism; the part of the BOLD signal that we analyze is dominated by a signal induced by a change in cerebral blood flow (CBF) that overcompensates for changes in the cerebral metabolic rate of oxygen consumption ($CMRO_2$) (Buxton et al., 2004). However, CBF and $CMRO_2$ are usually coupled (Hoge et al., 1999), suggesting that our measurements are positively correlated with metabolic demands. If adaptation is caused by an active hyperpolarization of cortical activity, this process is metabolically efficient, requiring less metabolic resources than simply maintaining activity related to stimuli that do not change.

Early experiments with contrast adaptation found that contrast gain shifts were present at the level of striate cortex, but not at the inputs from the lateral ge-

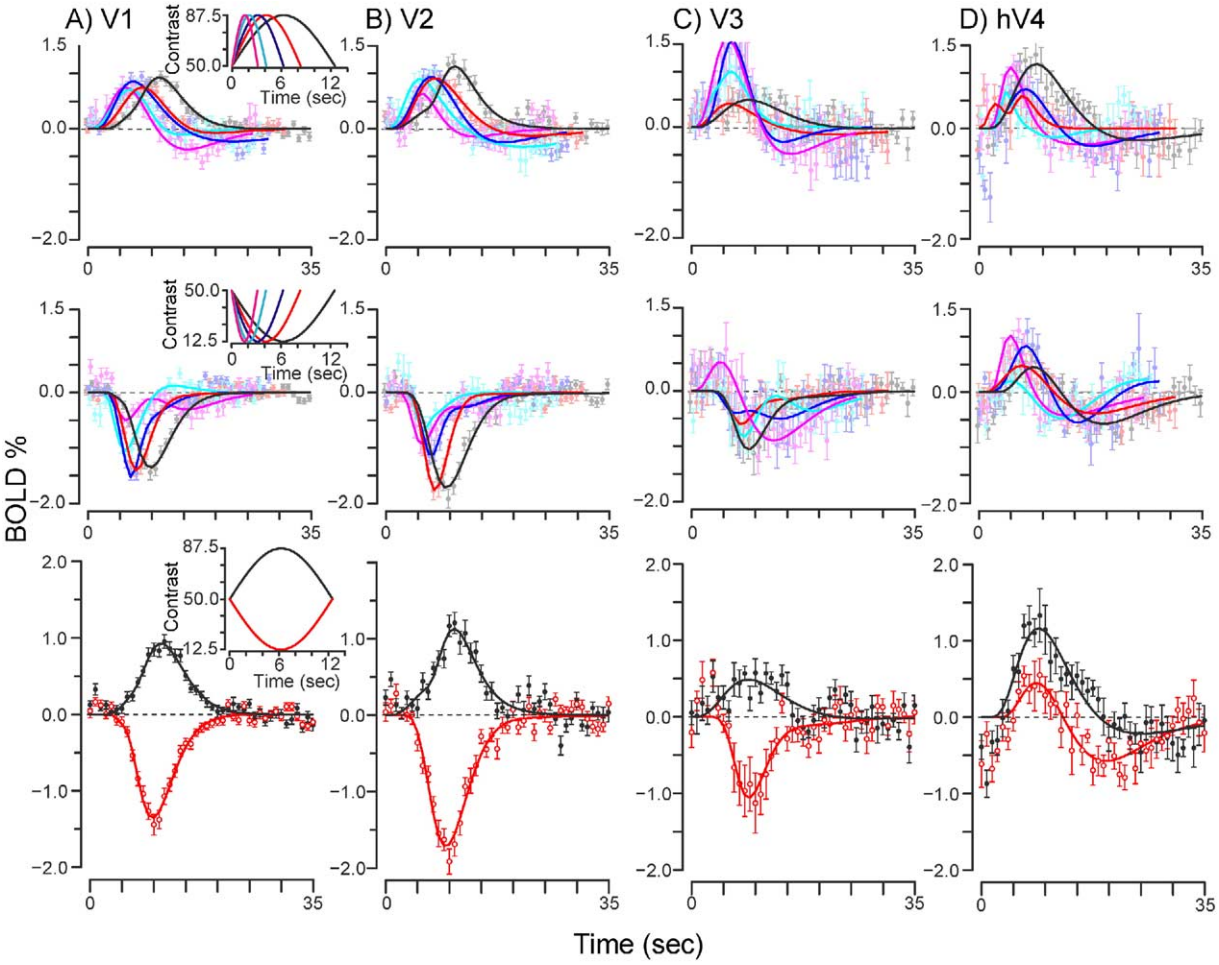

Figure 8. Positive Responses to Contrast Decrements in hV4 Examined with Different Stimulus Lengths

(A–D) For the regions indicated, each column represents the responses found to contrast increments (top row) or decrements (middle row) presented as one half-period of a sinusoidal modulation. Magenta, cyan, blue, red, and black traces and symbols represent the fit, mean, and standard error of the responses for 3.125, 4.167, 6.25, 8.3, and 12.5 s of stimulus duration, respectively. Insets in the first column display stimulus types. Bottom row replots the response to the longest stimulus duration (12.5 s) for both contrast increments (black) and decrements (red) to facilitate comparison between the two.

niculate nucleus (LGN) (Bonds, 1991; Ohzawa et al., 1982), suggesting that the adaptation in the BOLD signal that we measure is not due to feed-forward synaptic input, but rather to neuronal firing and recurrent feedback. However, more recent findings have suggested that contrast adaptation may not be specific to cortical processing, but may also occur in the LGN (Shou et al., 1996), particularly in the magnocellular division, (Solomon et al., 2004) as well as the retina (Chander and Chichilnisky, 2001; Smirnakis et al., 1997). While it would be of interest to know whether contrast gain changes occur in the human LGN, our slice prescription and imaging procedures were optimized for V1 and would require further retooling and optimization to record useful signals from the LGN (Chen et al., 1998; Kastner et al., 2004).

Relation to Previous Experiments

Although reports of experiments in anesthetized cats (Bonds, 1991; Ohzawa et al., 1982, 1985; Sclar et al., 1985) have described contrast gain changes with adaptation to contrast, some human imaging experiments (Kastner et al., 2004) have not found contrast adaptation, while others (Engel and Furmanski, 2001) have. Our experiments have uncovered robust contrast gain changes that very nearly center contrast-response functions on the adapting contrast, closely mirroring the cat data in terms of contrast gain (Ohzawa et al., 1982) and rate of adaptation (Albrecht et al., 1984). While individual neurons in single-unit studies may exhibit a range of susceptibility to adaptation (Sclar et al., 1989), our measurements are sensitive to the activity of large populations of neurons and therefore indicate that, on the whole, contrast gain changes shift contrast response to the range that is functionally beneficial. Previous block design imaging experiments (Kastner et al., 2004), which have compared contrast response functions measured with ascending versus descending contrasts, may not have been as sensitive to adaptation changes as are event-related studies (this study and Engel and

Furmanski, 2001). Changes in BOLD contrast response functions have been noted in surround suppression experiments (Zenger-Landolt and Heeger, 2003), sharing some similarities with the effect that we find with adaptation. However, surround suppression induces more response-gain changes that are likely to be mediated by neurons with different receptive field locations. Finally, the contrast gain changes that we have documented are closely paralleled by psychophysical measurements (Greenlee et al., 1991; Greenlee and Heitger, 1988). These psychophysical findings demonstrate that adaptation results in the lowering of contrast discrimination thresholds near the adapting contrast, but at the expense of discrimination at lower contrasts, just as would be predicted by our findings.

Our results have implications for previous measurements of contrast sensitivity using fMRI, which have typically used longer block designs. Given the time constants of adaptation that we found (median, ~14 s), long blocks of stimulation may confound contrast sensitivity with adaptation. In fact, our measurements of contrast sensitivity before and after adaptation indicate that block design experiments (depending on the length of the block) could, in the limit, result in a greater than 3-fold underestimation of contrast sensitivity. Accurate measurements of contrast sensitivity are particularly important for studies relating BOLD measurements to behavior (Boynton et al., 1999; Zenger-Landolt and Heeger, 2003) or to levels of neural activity (Heeger et al., 2000). Moreover, when comparing contrast sensitivity across areas (Avidan et al., 2002), differences in adaptation rates may result in mistakes in the estimation of contrast sensitivities. Adaptation rates have been found to increase with higher-order areas (Tolias et al., 2001), suggesting that decreases in contrast sensitivity may, in part, be due to differences in rates of adaptation.

Functional Baseline

Our method for constructing contrast response functions relies on both steady-state and transient BOLD responses; thus, we implicitly assume that it is valid to combine these two types of measurements. If the hemodynamic response itself undergoes adaptation, our results may overestimate the amount of neural adaptation that has occurred. However, this is generally not thought to be the case (Bandettini et al., 1997). Moreover, the time constants of the adaptation that we observed are very similar to those reported from single-unit studies, thus supporting our interpretation of neural, and not hemodynamic, adaptation.

Our study uses both positive and negative BOLD responses that may not be directly comparable. Indeed, we have noted some differences in the temporal dynamics of the two (Gardner et al., 2005). However, there is no evidence that the magnitudes of these positive and negative BOLD responses correspond to different magnitude changes of neural responses. Even if this were the case, differences in the magnitude of positive and negative BOLD responses would be expected to affect all of our contrast response functions, thus changing the shape of the curves, but not the horizontal shift with adaptation.

The comparison of transient to sustained baseline responses is not limited to our study or to adaptation studies in general, but is ubiquitous among fMRI studies. For example, testing the response to a visual stimulus from a neutral background assumes that the neutral background gives the natural baseline response for visual cortex, an assumption that is debatable (Gusnard and Raichle, 2001). While studies have manipulated the hemodynamic baseline pharmacologically (Hyder et al., 2002) or through hypercapnia (Cohen et al., 2002) to examine the consequences for transient responses, it is not clear if these artificial interventions are relevant to natural changes in baseline. Our results provide a functionally relevant way to change baseline and therefore suggest that the baseline for visual cortex is an adaptive state, controlled in part by the cortex itself.

Contrast Representation in hV4 versus V1–V3

Our results indicated a fundamental difference between the response of V1–V3 and hV4 to contrast changes; hV4 responded with increased responses to both increments and decrements of contrast (cf. Engel, 2005). Only at a longer time scale did hV4 decrease its response to decrements in stimulus contrast. Previous lesion experiments have implicated monkey V4 as being especially important for detecting stimuli like decrements in contrast that are less salient than neighboring distractors (Schiller and Lee, 1991)—a task that shows benefits with spatially directed attention (Braun, 1994). Our results may be another signature of the same phenomenon, suggesting that hV4 does not faithfully represent contrast as earlier areas do, but signals the salience of changes in stimulus contrast.

This result for hV4 is not predicted by reports of task-related or attentional modulations in human visual cortex (Pessoa et al., 2003). We controlled attention across different stimulus types by having subjects perform a detection task on the fixation cross throughout the experiment. Even still, abrupt changes in stimulus contrast can capture spatial attention (Jonides and Yantis, 1988), and, therefore, our results may be explained as a form of transient attention. If so, it is very different than that in previous reports of modulations due to task contingencies and sustained (Brefczynski and DeYoe, 1999; Gandhi et al., 1999; Somers et al., 1999; Tootell et al., 1998; Watanabe et al., 1998) or transient attention (Liu et al., 2005), which have found large effects in early visual cortex, often including V1.

This type of response in hV4 that does not distinguish between increments and decrements in contrast may be functionally analogous to the way that complex cells in V1 signal both increments and decrements of luminance. It could, in principle, be achieved through rectification and summing or squaring of the output of neurons in earlier visual areas that show signed responses to contrast increments and decrements. However, there are no known cell classes analogous to on- and off-type LGN cells that respond with positive responses to contrast increments and decrements, respectively. It therefore seems likely that the synaptic mechanisms in hV4 that give rise to these responses are qualitatively different from those of V1 neurons and may involve

cortical feedback mechanisms rather than feedforward mechanisms.

This property that distinguishes hV4 from early visual cortex could be used as a functional marker that could help in defining the hierarchy of human visual areas (Brewer et al., 2005; Hadjikhani et al., 1998; McKeefry and Zeki, 1997) and in determining homologies to the monkey hierarchy.

Conclusion

In conclusion, our results demonstrate contrast gain changes in human cortex that roughly serve to center contrast response functions on the adaptation contrast, thus allowing neurons with limited dynamic range to represent the much larger range of contrasts present in the visual world. Contrast gain changes like those that we have measured represent a slow process that adjusts the sensitivity of neurons to unchanging, and therefore less informative, aspects of visual scenes. We have also discovered a complementary mechanism not present in visual areas earlier than hV4 that is sensitive to changes in contrast, regardless of the sign of the change. Differences in the timescale of changes in stimulus contrast can serve as a cue of their behavioral relevance. Things that change rapidly often signal events in the world that may be dangerous, like a predator, or potentially rewarding, like a prey. Slow changes may be due to lighting differences or otherwise uninformative aspects of the environment. Our study demonstrates two mechanisms in the human visual system, one that makes contrast gain adjustments so as to be insensitive to slow changes in overall contrast, and another that is sensitive to rapid changes in contrast that could signal informative events.

Experimental Procedures

Human Subjects

We studied the occipital cortex of five healthy male subjects, two of which are authors (29–41 years of age). All procedures were approved in advance by the RIKEN Functional MRI Safety and Ethics Committee, and subjects gave prior written informed consent before each experiment.

Imaging Hardware

All experiments were conducted on a Varian Unity Inova 4 Tesla whole-body MRI system (Varian NMR Instruments, Palo Alto, CA) equipped with a Magnex head gradient system (Magnex Scientific Ltd., Abingdon, UK). High-resolution 3D T1-weighted anatomical MR images were scanned with a bird-cage radio-frequency (RF) coil or a transverse electromagnetic RF coil. A 5 inch transmit/receive butterfly quadrature RF surface coil was used to acquire functional (T2*-weighted) and coregistered anatomical (T1-weighted) images.

Rigid head motion was monitored with two pressure sensors and restricted by requiring subjects to use a bite-bar. Heartbeat was monitored with a pulse oximeter, and respiration with a pressure sensor. Both signals were recorded along with the timing of RF pulses for later corrections of physiological fluctuations.

Visual Stimulation

Visual stimuli were generated on a Macintosh computer, using the Psychophysics Toolbox (Brainard, 1997; Pelli, 1997) running on Matlab 5.2.1 (Mathworks, Natick, MA) and were displayed via an optic fiber goggle system (Avotec Inc., Jensen Beach, FL) that subtended 30° × 23° of visual angle. Subjects adjusted two refractive correction lenses on the goggle system to achieve corrected-to-normal vision. The luminosity of the brightest white achievable on the goggles was ~4 lux and the darkest black was ~0.5 lux. The goggles were gamma-corrected using a value of gamma estimated with a psychophysical procedure from the Psychophysics Toolbox.

The stimulus sequence began with 30 s of fixation during which the subject viewed a gray screen (Figure 1). To help maintain fixation and evenly allocate attention, the subject performed a moderately demanding detection task on the fixation cross throughout the whole experiment. Every 3 to 5 s, the fixation cross would turn red for 100 ms, and the subject was to report that event with a button press. We nevertheless monitored the subject's eye position using iView (SensoMotoric Instruments, Boston, MA) and the eye tracker built into the goggle system. Offline analysis confirmed that the subjects maintained fixation throughout the experiment. After the initial baseline period, an adaptation stimulus, which consisted of four 8° diameter stimuli placed 7° diagonally away from the fixation point, was presented for 60 s. The checkerboards had a checker size of 1° and flickered at 7.5 Hz. We split the stimuli into four quadrants, avoiding the fovea and the horizontal and vertical meridians to aid with later retinotopic mapping. The stimulus contrast defined as the difference in luminance between the bright and dark squares divided by the sum (and multiplied by 100) was set to an adaptation level of 6.25%, 12.5%, or 25%. After this initial adaptation period, we randomly interleaved 3 s test stimuli that had a contrast 1 or 2 octaves above or below the adaptation contrast, but were otherwise identical to the adaptation stimulus. These test contrasts were presented at least 15 times in random order during each experiment (duration, ~16 min). Between each test contrast, we presented the adaptation contrast again for 8–12 s to maintain the adaptation level.

Imaging Parameters

We collected eight slices perpendicular to the calcarine sulcus. Anatomical images were collected with a four-segment T1-weighted FLASH sequence. Functional images were acquired with a two-segment centric-ordered EPI sequence with a volume TR of 0.8 s (100 ms per slice) and a TE of 25 ms. Functional images were 4 mm thick and had an in-plane resolution of either 3.75 × 3.75 mm^2 (field of view [FOV] = 24 × 24 cm^2, matrix size = 64 × 64) for the contrast adaptation experiments (Figures 1–7) or 3.125 × 3.125 mm^2 (FOV = 20 × 20 cm^2, matrix size = 64 × 64) for the contrast sinusoid experiments (Figure 8). Longitudinal magnetization was allowed to reach steady state before EPI images were collected. A full volume without phase encoding was taken at the beginning of the sequence and used to correct for phase errors (Bruder et al., 1992). The first echo in each segment was a navigator echo used to correct intersegment phase and amplitude variations (Kim et al., 1996).

Data Processing and Analysis

After EPI image reconstruction, cardiac and respiratory fluctuations were further removed using a retrospective estimation and correction method (Hu et al., 1995), and motion correction was applied (Maas et al., 1997), both in k-space. A high-pass filter with a cutoff of 0.004 Hz (but set to retain the DC) was then used to suppress slow signal drifts caused by noise. The event-related responses were sufficiently high frequency to be largely unaffected by this filter. However, the initial decay (Figure 6) could have been accentuated by the filtering. Analysis of data without filtering resulted in qualitatively similar exponential decay and did not substantially affect our results. All further analyses after these preprocessing steps were performed with custom-built software in Matlab 6.5.

We computed estimated hemodynamic response functions for each stimulus in individual voxels without making any assumptions about the shape of the hemodynamic response. We assumed the following model of the BOLD time course, in block matrix format:

$$[S_1 \;\; S_2 \;\; \ldots \;\; S_n] \times [H_1 \;\; H_2 \;\; \ldots \;\; H_n]^T + \text{noise} = [\text{BOLD}]^T \qquad (1)$$

where, S_i is the i^{th} stimulus convolution matrix and has dimensions M × N, where M is the number of time points in the time course and N is the number of time points for which we calculate the estimated hemodynamic response. (We calculate 20 s of response, which for a TR of 0.8 s contains 25 time points.) Each H_i is a 1 × N array of the unknown hemodynamic response to the i^{th} stimulus. T is the transpose operation. Noise is assumed to be zero-mean Gaussian.

BOLD is a 1 × M array that contains a mean subtracted time series for the voxel. We then computed the hemodynamic responses (H_i) to each stimuli at each voxel that minimized the squared error between the left and right sides of equation 1. We randomized interstimulus times so that, in addition to sampling different combinations of responses to the different stimuli, we would also sample different temporal combinations (Burock et al., 1998). We also attempted to reduce estimation errors due to violations of temporal linearity by separating stimuli in time by a longer time interval than the main positive part of the hemodynamic response (i.e., 8–12 s). Raw imaging values were converted to percent modulations by dividing the time courses by the average response during the baseline period. 0% modulation was set to the mean during the experiment.

We developed a statistical analysis that used the event-related responses in each voxel without reference to a separate localizer to evaluate activation. Our analysis asks what percentage of the variance in the BOLD response can be accounted for by events that are time-locked to stimulus presentations. We first generated an estimated time course by multiplying the stimulus convolution matrices with the estimated hemodynamic responses. We then computed the amount of variance in the original time course that is accounted for by this estimate (r^2):

$$r^2 = 1 - \frac{\text{variance (residual)}}{\text{variance (original)}} \quad (2)$$

where the residual was the difference between the estimated and original time courses.

To estimate the statistical significance of a particular value of r^2, we used a permutation procedure. We randomized the stimulus times so that they were no longer time-locked to stimulus events. We then recalculated hemodynamic responses for every voxel in the volume, using deconvolution and then recalculated r^2 values. We took this distribution of r^2 values (randomized distribution) to represent the distribution of r^2 values that would be expected by chance correlations of noise with stimulus times. The tail of the real r^2 distribution had many larger values of r^2 than the randomized distribution, which we took to be voxels that were significantly activated. We then computed p values based on the randomized distribution by finding a cutoff that included only a desired amount of noise voxels—for example, 0.1%, by picking the r^2 value of the voxel that ranked as the 99.9% highest r^2 value in the randomized distribution. With a cutoff chosen in this way, we expect in the real data to have 0.1% of the voxels deemed activated to be actually noise voxels with spurious correlations with the stimulus times (Figure 3). The cutoff value was determined for each scan individually.

To quantify the magnitude of activation to each stimulus type, we used the maximum value of a gamma function that was fit to the data:

$$A\frac{(\frac{t-lag}{\tau})^{n-1}e^{-\frac{t-lag}{\tau}}}{\tau(n-1)!} \quad (3)$$

where A is the amplitude; n is a shape parameter allowed to take on integer values from 4 to 6; and τ roughly corresponds to the width of the response and was allowed to take on values from 0.5 to 2 s. The *lag* value, which controls when the gamma function begins relative to stimulus onset, took on values ranging from 0 to 4 s. When *t-lag* was negative, the function was set to 0. A difference of gamma functions (Equation 3), in which the second gamma function was allowed to have τ values between 0.5 and 4 s and a *lag* 2–8 s, was used to capture the delayed negative response of the hemodynamic function.

We fit the gamma functions by first making an estimated time course in which each stimulus occurrence was replaced by a gamma function (for each stimulus type we used a separate set of parameters). Any overlap in the gamma functions from one stimulus to the next was assumed to sum linearly. We then used Levenberg-Marquardt optimization to find the parameters of each gamma function that minimized the mean squared difference between the estimated time course and the actual time course. Our stimulus presentation times were intentionally not synched to volume acquisition so that on different stimulus presentations, different time points relative to the stimulus onset would be sampled. Furthermore, our multi-shot protocol was not interleaved across slices so that we could use the actual time of slice acquisition instead of the volume TR to get better time resolution of the response.

We fit contrast response curves with the following equation:

$$\text{Response} = R_{max}\frac{\text{contrast}^n}{\text{contrast}^n + {c_{50}}^n} + \text{offset} \quad (4)$$

where R_{max} is the maximum amplitude, c_{50} is the contrast at which the curve reaches half height, and n controls the steepness. To avoid overfitting, we set n to 2. Offset was unconstrained, while R_{max} and c_{50} were positive values. 0% BOLD for the contrast response functions is taken as the response during the baseline condition.

To estimate the rate of adaptation, we fit a decaying exponential to the initial portion of the response:

$$Ae^{-\frac{t}{\tau}} + \text{offset} \quad (5)$$

where A is the amplitude and τ is the time constant.

Retinotopy

We defined ROIs for different visual areas with an event-related stimulus paradigm in which we presented 45° wide wedges of flickering checkerboards either along the horizontal or vertical meridian (randomly interleaved) for 3 s (cf. Engel et al., 1994; Sereno et al., 1995). Each stimulus presentation was followed by 4–8 s of gray. We computed hemodynamic responses and mapped the meridians as the difference between the peak response to the horizontal and vertical stimuli. We then marked the visual regions as areas that extended from one meridian to the next along the gray matter, using BrainVoyager (Brain Innovation, Maastricht, The Netherlands). We combined the dorsal and ventral aspects of V1–V3 since we did not see significant differences between them (though our slice positioning tended to oversample the ventral areas). Human V4 (hV4) was defined as the ventral visual area that continues laterally from V3. This area, typically located on the medial lip of the collateral sulcus but avoiding the depth of the sulcus, corresponds mostly to V4v defined in other retinotopic studies (Hadjikhani et al., 1998; Sereno et al., 1995). These ROIs and each functional data set were then registered to a 3D anatomical image of the whole brain. We determined whether a voxel was in a particular visual area in a strict fashion by requiring that the voxel overlap with the ROI for that visual area and not with any other ROI.

Acknowledgments

J.L.G. and P.S. were supported by postdoctoral fellowships from the Japan Society for the Promotion of Science. J.L.G. was also supported by a National Research Service Award (1F32EY016260-01). We thank I-han Chou, David Heeger, and the members of the Heeger lab for helpful discussions.

Received: February 24, 2005
Revised: June 7, 2005
Accepted: July 19, 2005
Published: August 17, 2005

References

Adorjan, P., Piepenbrock, C., and Obermayer, K. (1999). Contrast adaptation and infomax in visual cortical neurons. Rev. Neurosci. *10*, 181–200.

Albrecht, D.G., and Hamilton, D.B. (1982). Striate cortex of monkey and cat: contrast response function. J. Neurophysiol. *48*, 217–237.

Albrecht, D.G., Farrar, S.B., and Hamilton, D.B. (1984). Spatial contrast adaptation characteristics of neurones recorded in the cat's visual cortex. J. Physiol. *347*, 713–739.

Allison, J.D., Casagrande, V.A., Debruyn, E.J., and Bonds, A.B.

(1993). Contrast adaptation in striate cortical neurons of the nocturnal primate bush baby (Galago crassicaudatus). Vis. Neurosci. *10*, 1129–1139.

Anzai, A., Bearse, M.A., Jr., Freeman, R.D., and Cai, D. (1995). Contrast coding by cells in the cat's striate cortex: monocular vs. binocular detection. Vis. Neurosci. *12*, 77–93.

Avidan, G., Harel, M., Hendler, T., Ben-Bashat, D., Zohary, E., and Malach, R. (2002). Contrast sensitivity in human visual areas and its relationship to object recognition. J. Neurophysiol. *87*, 3102–3116.

Bandettini, P.A., Kwong, K.K., Davis, T.L., Tootell, R.B., Wong, E.C., Fox, P.T., Belliveau, J.W., Weisskoff, R.M., and Rosen, B.R. (1997). Characterization of cerebral blood oxygenation and flow changes during prolonged brain activation. Hum. Brain Mapp. *5*, 93–109.

Blakemore, C., and Campbell, F.W. (1969). On the existence of neurones in the human visual system selectively sensitive to the orientation and size of retinal images. J. Physiol. *203*, 237–260.

Bonds, A.B. (1991). Temporal dynamics of contrast gain in single cells of the cat striate cortex. Vis. Neurosci. *6*, 239–255.

Boynton, G.M., Engel, S.A., Glover, G.H., and Heeger, D.J. (1996). Linear systems analysis of functional magnetic resonance imaging in human V1. J. Neurosci. *16*, 4207–4221.

Boynton, G.M., Demb, J.B., Glover, G.H., and Heeger, D.J. (1999). Neuronal basis of contrast discrimination. Vision Res. *39*, 257–269.

Brainard, D.H. (1997). The psychophysics toolbox. Spat. Vis. *10*, 433–436.

Braun, J. (1994). Visual search among items of different salience: removal of visual attention mimics a lesion in extrastriate area V4. J. Neurosci. *14*, 554–567.

Brefczynski, J.A., and DeYoe, E.A. (1999). A physiological correlate of the 'spotlight' of visual attention. Nat. Neurosci. *2*, 370–374.

Brewer,, A.A., Liu, J., Wade, A.R., and Wandell, B.A. (2005). Visual field maps and stimulus selectivity in human ventral occipital cortex. Nat. Neurosci. *8*, 1102–1109.

Bruder, H., Fischer, H., Reinfelder, H.E., and Schmitt, F. (1992). Image reconstruction for echo planar imaging with nonequidistant k-space sampling. Magn. Reson. Med. *23*, 311–323.

Burock, M.A., Buckner, R.L., Woldorff, M.G., Rosen, B.R., and Dale, A.M. (1998). Randomized event-related experimental designs allow for extremely rapid presentation rates using functional MRI. Neuroreport *9*, 3735–3739.

Buxton, R.B., Uludag, K., Dubowitz, D.J., and Liu, T.T. (2004). Modeling the hemodynamic response to brain activation. Neuroimage *23* (*Suppl 1*), S220–S233.

Carandini, M., and Ferster, D. (1997). A tonic hyperpolarization underlying contrast adaptation in cat visual cortex. Science *276*, 949–952.

Carandini, M., Barlow, H.B., O'Keefe, L.P., Poirson, A.B., and Movshon, J.A. (1997). Adaptation to contingencies in macaque primary visual cortex. Philos. Trans. R. Soc. Lond. B Biol. Sci. *352*, 1149–1154.

Chance, F.S., Nelson, S.B., and Abbott, L.F. (1998). Synaptic depression and the temporal response characteristics of V1 cells. J. Neurosci. *18*, 4785–4799.

Chander, D., and Chichilnisky, E.J. (2001). Adaptation to temporal contrast in primate and salamander retina. J. Neurosci. *21*, 9904–9916.

Chen, W., Kato, T., Zhu, X.H., Strupp, J., Ogawa, S., and Ugurbil, K. (1998). Mapping of lateral geniculate nucleus activation during visual stimulation in human brain using fMRI. Magn. Reson. Med. *39*, 89–96.

Cohen, E.R., Ugurbil, K., and Kim, S.G. (2002). Effect of basal conditions on the magnitude and dynamics of the blood oxygenation level-dependent fMRI response. J. Cereb. Blood Flow Metab. *22*, 1042–1053.

Dale, A.M., and Buckner, R.L. (1997). Selective averaging of rapidly presented individual trials using fMRI. Hum. Brain Mapp. *5*, 329–340.

Dean, A.F. (1981). The relationship between response amplitude and contrast for cat striate cortical neurones. J. Physiol. *318*, 413–427.

Dean, A.F. (1983). Adaptation-induced alteration of the relation between response amplitude and contrast in cat striate cortical neurones. Vision Res. *23*, 249–256.

Dougherty, R.F., Koch, V.M., Brewer, A.A., Fischer, B., Modersitzki, J., and Wandell, B.A. (2003). Visual field representations and locations of visual areas V1/2/3 in human visual cortex. J. Vis. *3*, 586–598.

Engel, S.A. (2005). Adaptation of oriented and unoriented color-selective neurons in human visual areas. Neuron *45*, 613–623.

Engel, S.A., and Furmanski, C.S. (2001). Selective adaptation to color contrast in human primary visual cortex. J. Neurosci. *21*, 3949–3954.

Engel, S.A., Rumelhart, D.E., Wandell, B.A., Lee, A.T., Glover, G.H., Chichilnisky, E.J., and Shadlen, M.N. (1994). fMRI of human visual cortex. Nature *21*, 525.

Finlayson, P.G., and Cynader, M.S. (1995). Synaptic depression in visual cortex tissue slices: an in vitro model for cortical neuron adaptation. Exp. Brain Res. *106*, 145–155.

Gandhi, S.P., Heeger, D.J., and Boynton, G.M. (1999). Spatial attention affects brain activity in human primary visual cortex. Proc. Natl. Acad. Sci. USA *96*, 3314–3319.

Gardner, J.L., Sun, P., Waggoner, R.A., Ueno, K., Tanaka, K., and Cheng, K. (2005). Differences in temporal dynamics of positive and negative BOLD responses. In Proceedings of the International Society for Magnetic Resonance in Medicine, May, 2005, Miami, FL 13, 25.

Greenlee, M.W., and Heitger, F. (1988). The functional role of contrast adaptation. Vision Res. *28*, 791–797.

Greenlee, M.W., Georgeson, M.A., Magnussen, S., and Harris, J.P. (1991). The time course of adaptation to spatial contrast. Vision Res. *31*, 223–236.

Gusnard, D.A., and Raichle, M.E. (2001). Searching for a baseline: functional imaging and the resting human brain. Nat. Rev. Neurosci. *2*, 685–694.

Hadjikhani, N., Liu, A.K., Dale, A.M., Cavanagh, P., and Tootell, R.B. (1998). Retinotopy and color sensitivity in human visual cortical area V8. Nat. Neurosci. *1*, 235–241.

Hammond, P., Mouat, G.S., and Smith, A.T. (1985). Motion after-effects in cat striate cortex elicited by moving gratings. Exp. Brain Res. *60*, 411–416.

Heeger, D.J., Huk, A.C., Geisler, W.S., and Albrecht, D.G. (2000). Spikes versus BOLD: what does neuroimaging tell us about neuronal activity? Nat. Neurosci. *3*, 631–633.

Hoge, R.D., Atkinson, J., Gill, B., Crelier, G.R., Marrett, S., and Pike, G.B. (1999). Linear coupling between cerebral blood flow and oxygen consumption in activated human cortex. Proc. Natl. Acad. Sci. USA *96*, 9403–9408.

Hu, X., Le, T.H., Parrish, T., and Erhard, P. (1995). Retrospective estimation and correction of physiological fluctuation in functional MRI. Magn. Reson. Med. *34*, 201–212.

Hyder, F., Rothman, D.L., and Shulman, R.G. (2002). Total neuroenergetics support localized brain activity: implications for the interpretation of fMRI. Proc. Natl. Acad. Sci. USA *99*, 10771–10776.

Jonides, J., and Yantis, S. (1988). Uniqueness of abrupt visual onset in capturing attention. Percept. Psychophys. *43*, 346–354.

Kastner, S., O'Connor, D.H., Fukui, M.M., Fehd, H.M., Herwig, U., and Pinsk, M.A. (2004). Functional imaging of the human lateral geniculate nucleus and pulvinar. J. Neurophysiol. *91*, 438–448.

Kim, S.G., Hu, X., Adriany, G., and Ugurbil, K. (1996). Fast interleaved echo-planar imaging with navigator: high resolution anatomic and functional images at 5 Tesla. Magn. Reson. Med. *35*, 895–902.

Kohn, A., and Movshon, J.A. (2003). Neuronal adaptation to visual motion in area MT of the macaque. Neuron *39*, 681–691.

Kruger, G., Kleinschmidt, A., and Frahm, J. (1996). Dynamic MRI

sensitized to cerebral blood oxygenation and flow during sustained activation of human visual cortex. Magn. Reson. Med. *35*, 797–800.

Liu, T., Pestilli, F., and Carrasco, M. (2005). Transient attention enhances perceptual performance and FMRI response in human visual cortex. Neuron *45*, 469–477.

Logothetis, N.K., Pauls, J., Augath, M., Trinath, T., and Oeltermann, A. (2001). Neurophysiological investigation of the basis of the fMRI signal. Nature *412*, 150–157.

Maas, L.C., Frederick, B.D., and Renshaw, P.F. (1997). Decoupled automated rotational and translational registration for functional MRI time series data: the DART registration algorithm. Magn. Reson. Med. *37*, 131–139.

Mandeville, J.B., Marota, J.J., Kosofsky, B.E., Keltner, J.R., Weissleder, R., Rosen, B.R., and Weisskoff, R.M. (1998). Dynamic functional imaging of relative cerebral blood volume during rat forepaw stimulation. Magn. Reson. Med. *39*, 615–624.

McKeefry, D.J., and Zeki, S. (1997). The position and topography of the human colour centre as revealed by functional magnetic resonance imaging. Brain *120*, 2229–2242.

Movshon, J.A., and Lennie, P. (1979). Pattern-selective adaptation in visual cortical neurones. Nature *278*, 850–852.

Naka, K.I., and Rushton, W.A. (1966). S-potentials from colour units in the retina of fish (Cyprinidae). J. Physiol. *185*, 536–555.

Ohzawa, I., Sclar, G., and Freeman, R.D. (1982). Contrast gain control in the cat visual cortex. Nature *298*, 266–268.

Ohzawa, I., Sclar, G., and Freeman, R.D. (1985). Contrast gain control in the cat's visual system. J. Neurophysiol. *54*, 651–667.

Pelli, D.G. (1997). The VideoToolbox software for visual psychophysics: transforming numbers into movies. Spat. Vis. *10*, 437–442.

Pessoa, L., Kastner, S., and Ungerleider, L.G. (2003). Neuroimaging studies of attention: from modulation of sensory processing to top-down control. J. Neurosci. *23*, 3990–3998.

Sanchez-Vives, M.V., Nowak, L.G., and McCormick, D.A. (2000a). Cellular mechanisms of long-lasting adaptation in visual cortical neurons in vitro. J. Neurosci. *20*, 4286–4299.

Sanchez-Vives, M.V., Nowak, L.G., and McCormick, D.A. (2000b). Membrane mechanisms underlying contrast adaptation in cat area 17 in vivo. J. Neurosci. *20*, 4267–4285.

Schiller, P.H., and Lee, K. (1991). The role of the primate extrastriate area V4 in vision. Science *251*, 1251–1253.

Sclar, G., Ohzawa, I., and Freeman, R.D. (1985). Contrast gain control in the kitten's visual system. J. Neurophysiol. *54*, 668–675.

Sclar, G., Lennie, P., and DePriest, D.D. (1989). Contrast adaptation in striate cortex of macaque. Vision Res. *29*, 747–755.

Sereno, M.I., Dale, A.M., Reppas, J.B., Kwong, K.K., Belliveau, J.W., Brady, T.J., Rosen, B.R., and Tootell, R.B. (1995). Borders of multiple visual areas in humans revealed by functional magnetic resonance imaging. Science *268*, 889–893.

Shou, T., Li, X., Zhou, Y., and Hu, B. (1996). Adaptation of visually evoked responses of relay cells in the dorsal lateral geniculate nucleus of the cat following prolonged exposure to drifting gratings. Vis. Neurosci. *13*, 605–613.

Smirnakis, S.M., Berry, M.J., Warland, D.K., Bialek, W., and Meister, M. (1997). Adaptation of retinal processing to image contrast and spatial scale. Nature *386*, 69–73.

Solomon, S.G., Peirce, J.W., Dhruv, N.T., and Lennie, P. (2004). Profound contrast adaptation early in the visual pathway. Neuron *42*, 155–162.

Somers, D.C., Dale, A.M., Seiffert, A.E., and Tootell, R.B. (1999). Functional MRI reveals spatially specific attentional modulation in human primary visual cortex. Proc. Natl. Acad. Sci. USA *96*, 1663–1668.

Tolhurst, D.J., Movshon, J.A., and Thompson, I.D. (1981). The dependence of response amplitude and variance of cat visual cortical neurones on stimulus contrast. Exp. Brain Res. *41*, 414–419.

Tolias, A.S., Smirnakis, S.M., Augath, M.A., Trinath, T., and Logothetis, N.K. (2001). Motion processing in the macaque: revisited with functional magnetic resonance imaging. J. Neurosci. *21*, 8594–8601.

Tootell, R.B., Reppas, J.B., Kwong, K.K., Malach, R., Born, R.T., Brady, T.J., Rosen, B.R., and Belliveau, J.W. (1995). Functional analysis of human MT and related visual cortical areas using magnetic resonance imaging. J. Neurosci. *15*, 3215–3230.

Tootell, R.B., Hadjikhani, N., Hall, E.K., Marrett, S., Vanduffel, W., Vaughan, J.T., and Dale, A.M. (1998). The retinotopy of visual spatial attention. Neuron *21*, 1409–1422.

Vautin, R.G., and Berkley, M.A. (1977). Responses of single cells in cat visual cortex to prolonged stimulus movement: neural correlates of visual aftereffects. J. Neurophysiol. *40*, 1051–1065.

Watanabe, T., Sasaki, Y., Miyauchi, S., Putz, B., Fujimaki, N., Nielsen, M., Takino, R., and Miyakawa, S. (1998). Attention-regulated activity in human primary visual cortex. J. Neurophysiol. *79*, 2218–2221.

Zenger-Landolt, B., and Heeger, D.J. (2003). Response suppression in v1 agrees with psychophysics of surround masking. J. Neurosci. *23*, 6884–6893.